Robustness of single-qubit geometric gate against systematic error

J. T. Thomas, Mahmoud Lababidi, and Mingzhen Tian
School of Physics, Astronomy and Computational Sciences, George Mason University, Fairfax, Virginia 22030, USA
(Received 30 June 2010; revised manuscript received 4 August 2011; published 24 October 2011)

Universal single-qubit gates are constructed from a basic Bloch rotation operator realized through nonadiabatic Abelian geometric phase. The driving Hamiltonian in a generic two-level model is parameterized using controllable physical variables. The fidelity of the basic geometric rotation operator is investigated in the presence of systematic error in control parameters, such as the driving pulse area and frequency detuning. Compared to a conventional dynamic rotation, the geometric rotation shows improved fidelity.

DOI: 10.1103/PhysRevA.84.042335 PACS number(s): 03.67.Pp, 03.67.Lx, 03.65.Vf

I. INTRODUCTION

In the implementation of scalable quantum information processing, a key challenge is to achieve controlled quantum state preparation and manipulation with high fidelity in the presence of imperfections. In the commonly adapted quantum computing circuit model [1], this requires a set of robust universal quantum gates. Quantum gates degrade due to both imperfections in the control Hamiltonian and decoherence in the physical qubit system during the gate operation. When the operation time is kept much shorter than the qubit coherence time, the systematic error and random noise in the control Hamiltonian become the dominant causes for the operation error [2]. The quality of a quantum gate is usually characterized by gate fidelity or error rate per gate. A scalable computation can be achieved through quantum error correction [3], provided the error rate is smaller than a certain threshold, usually 10^{-4}, or a fidelity above 99.999% [2,4].

In recent years various all-geometric schemes based on quantum holonomy have been considered effective ways to minimize the operation errors caused by random noise. A control Hamiltonian is designed to drive a qubit along a specific path so that the resulting state transformation is affected only by the global geometry of the quantum system, not by the details of the evolution paths that are usually fluctuating due to noises in the control Hamiltonian [5–13]. The all-geometric approaches existing so far utilize either Abelian- or non-Abelian holonomy, which results in the state transformation expressed as a phase change or a unitary matrix, respectively. The non-Abelian geometric approach, usually called holonomic quantum computation [5], has been considered as a novel quantum computation model and proven fault tolerant under the adiabatic condition [14]. In the circuit model, holonomic quantum gates have been investigated for robustness against random parametric noise, most of them in adiabatic cases [15], which requires a long operation time. Breaking the adiabatic limit to shorten the operation time brings the quantum gates into no pure-geometric regimes [16]. Non-Abelian quantum gates have not been experimentally demonstrated mainly due to the difficulties in manipulation and measurement of multiple degenerate quantum states. On the other hand, the Abelian all-geometric approach is relatively simple since the gate operations are performed on nondegenerate two-level qubits through either Berry's phase [17] in an adiabatic evolution or Aharonov-Anandan (A-A) phase [18] in a nonadiabatic process. Abelian geometric gates have been proposed and demonstrated in almost all viable qubit systems so far, including [8–13] NMR, cold atoms or ions, photons, superconducting circuits, quantum dots, cavity QED, and atomic ensembles in solids. The fault tolerance against errors in the control Hamiltonian is still under investigation, and fidelity analysis has been focused on the effect of the random error [19–22]. The results, however, are still less conclusive for a general two-level system. In addition, the effects from seemingly simple systematic errors have not yet been addressed.

In this paper we focus on the robustness of a type of nonadiabatic Abelian geometric gates against systematic errors in the control parameters. Based on A-A phase, two noncommutable basic Bloch rotations were previously proposed and experimentally demonstrated, which can be used to compose any universal single-qubit gate [12]. The Hamiltonians controlling the rotations are made of a special type of composite pulses that drive the eigenvectors of the system through closed paths in the projective Hilbert space (a Bloch sphere), eliminating the dynamic phase. This paper generalizes the basic rotations as a rotation operator that suffices for making any single-qubit gates. Since the two-level qubit and the driving Hamiltonian are parameterized as a Bloch vector and a torque vector, respectively, evolving on the Bloch sphere this scheme is applicable to a generic two-level qubit. We are able to use the rotation operator to analyze the gate fidelity, which is independent of the qubit state. The fidelity is calculated in the presence of systematic errors in the control parameters, such as pulse area and frequency detuning. The geometric rotation is compared with conventional dynamic rotation. The link between the geometricity and high operation fidelity is discussed.

II. UNIVERSAL QUANTUM GATES AND BASIC BLOCH ROTATION

The quantum state of a qubit $|\psi\rangle = \cos\frac{\alpha}{2}|0\rangle + e^{i\beta}\sin\frac{\alpha}{2}|1\rangle$ can be represented by a Bloch vector $\vec{r} = (\sin\alpha\cos\beta, \sin\alpha\sin\beta, \cos\alpha)$ on the Bloch sphere as shown in Fig. 1(a). The polar angle α varies from 0 to π and the azimuthal angle β from 0 to 2π. A rotation on the Bloch sphere represents a universal quantum gate that can be expressed as

$$U_{\vec{n}}(\theta) = \exp(-i\vec{\sigma}\cdot\vec{n}\theta/2) = \cos(\theta/2)I - i\sin(\theta/2)\vec{\sigma}\cdot\vec{n}, \quad (1)$$

 ©2011 American Physical Society

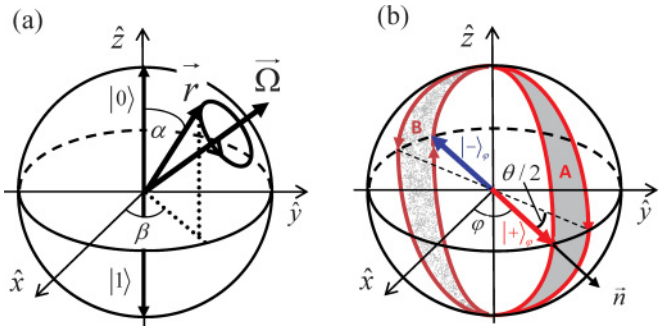

FIG. 1. (Color online) (a) Bloch vector $\vec{r}$ rotates around Rabi vector $\vec{\Omega}$ on the Bloch sphere. (b) Geometric paths A and B for basis vectors $|+\rangle_\varphi$ and $|-\rangle_\varphi$, respectively, to accomplish rotation $U(\theta,\varphi)$ in Eq. (2), where $\vec{n}$ is the rotation axis and θ the rotation angle.

where θ is the angle of rotation around axis $\vec{n}$, and I and $\vec{\sigma} = (\sigma_x,\sigma_y,\sigma_z)$ are the identity and Pauli matrices, respectively.

Since a rotation around an arbitrary axis can be made by rotations around two unparallel axes in the x-y plane, the problem of making a universal set of single-qubit gates reduces to making rotations around $\vec{n} = (\cos\varphi, \sin\varphi, 0)$ in the x-y plane, where φ is the angle between the x axis and the rotation axis $\vec{n}$. The rotation operator becomes

$$U(\theta,\varphi) = \cos(\theta/2)I - i\sin(\theta/2)(\cos\varphi\sigma_x + \sin\varphi\sigma_y), \quad (2)$$

where φ defines the rotation axis and θ the rotation angle. Any single-qubit gate can be made of at most three rotations characterized by such an operator with controllable φ and θ [23].

In a generic two-level model, the motion of the Bloch vector obeys the Bloch equation [24], $d\vec{r}/dt = \vec{\Omega} \times \vec{r}$, where the Bloch vector represents the quantum state and the driving Hamiltonian $H = (\hbar\Delta/2)\sigma_z + (\hbar\Omega_0/2)(\cos\varphi\sigma_x + \sin\varphi\sigma_y)$ in the rotating frame is parameterized by the torque given by the Rabi vector $\vec{\Omega}$. As shown in Fig. 1(a), the Bloch vector rotates around the driving torque by an angle of the pulse area $\theta = \Omega\tau$, where τ is the duration for a constant torque acting on the Bloch vector. The evolution of a two-level system, such as an atom or spin-1/2 particle, can be modeled as an effective dipole moment driven by an effective field near the resonance of the transition between the two energy levels of the qubit [24]. The driving field, $F(t) = \Omega_0\cos(\omega t + \phi)$, determines the Rabi vector to be $\Omega = (-\Omega_0\cos\phi, -\Omega_0\sin\phi, \Delta)$. The field amplitude Ω_0 is defined as Rabi frequency and takes into account the effective dipole moment; ϕ is the phase of the field; and Δ is the frequency detuning between the driving field and the resonance of the two-level system. These are the parameters that define the quantum gate operation and control the motion of the Bloch vector.

Conventionally, to make the rotation around an axis $\vec{n} = (\cos\varphi, \sin\varphi, 0)$ in the x-y plane as in Eq. (2), a pulse of an on-resonance field with constant amplitude Ω_0, phase $(\varphi + \pi)$, and duration τ is applied. A pulse with such parameters sets the Rabi vector $\Omega = (\Omega_0\cos\varphi, \Omega_0\sin\varphi, 0)$ along the desired rotation axis and the pulse area to the rotation angle $\theta = \Omega_0\tau$. The dynamic evolution driven by a simple pulse is ideal with 100% operation fidelity if the control parameters, including the Rabi frequency, phase, pulse length, and detuning, are perfect. However, when there is systematic error or random noise in the control parameters, this conventional simple pulse scheme may result in a high error rate and low fidelity.

III. SYSTEMATIC ERROR AND GATE FIDELITY

In the presence of error in the control parameters, an ideal operator U, such as in Eq. (2) turns into an imperfect operator V with erroneous rotation axis, angle, or both. Fidelity, usually used to evaluate the closeness of the two operators, is defined as [23,25,26]

$$F = |\mathrm{Tr}(VU^\dagger)|/2. \quad (3)$$

This allows us to study the fidelity of any quantum gate independent of the qubit state.

Systematic errors in the control parameters that affect the operation in Eq. (2) can be mainly categorized as pulse area error and frequency detuning error. The error in the pulse area $\theta = \Omega\tau$ is usually caused by inaccuracy in the Rabi frequency and the pulse duration. These result in an erroneous rotation angle. The detuning error due to the frequency difference between the driving pulse and the qubit resonance causes errors in the rotation axis and angle. Similar to the treatment for the composite pulse in NMR [27–29], we consider the pulse area and detuning errors separately.

The pulse area $\theta_\varepsilon = \theta(1+\varepsilon)$ with a percentage error ε corresponds to the operator $V(\theta,\varphi) = \exp(-i\vec{\sigma}\cdot\vec{n}\theta_\varepsilon/2)$. Using Eq. (3) the fidelity of such an operator is calculated to be

$$F_{s\varepsilon} = \cos(\varepsilon\theta/2), \quad (4)$$

in which the fidelity degrades with the pulse area error and the rotation angle in the range of $[-\pi,\pi]$. The error affects a large rotation angle more than a small angle. The fidelity is uniform for all rotation axes at a given error level and rotation angle.

In most of the cases the percentage error in pulse area is expected to be small, where $|\varepsilon| \ll 1$ holds and the fidelity approximates to

$$F_{s\varepsilon} \approx 1 - \frac{1}{2}\left(\frac{\theta}{2}\right)^2\varepsilon^2. \quad (5)$$

In the presence of the frequency detuning Δ, the Rabi frequency is generalized as $\Omega = \sqrt{\Omega_0^2 + \Delta^2} = \Omega_0\sqrt{1+f^2}$, where Ω_0 is on-resonance Rabi frequency and $f = \Delta/\Omega_0$ is the relative detuning with respect to Ω_0. The detuning affects both the rotation angle and the direction of the rotation axis. The ideal rotation angle θ turns into $\theta\sqrt{1+f^2}$ and the rotation axis $\vec{n} = (\cos\varphi, \sin\varphi, 0)$ shifts to $\vec{n}_f = (\frac{1}{\sqrt{1+f^2}}\cos\varphi, \frac{1}{\sqrt{1+f^2}}\sin\varphi, \frac{f}{\sqrt{1+f^2}})$. The rotation operator becomes

$$V(\theta,\varphi) = \cos\left(\frac{\theta\sqrt{1+f^2}}{2}\right)I - i\sin\left(\frac{\theta\sqrt{1+f^2}}{2}\right)\vec{\sigma}\cdot\vec{n}_f. \quad (6)$$

The corresponding fidelity is calculated to be

$$F_{\rm sf} = \cos\frac{\theta\sqrt{1+f^2}}{2}\cos\frac{\theta}{2} + \frac{1}{\sqrt{1+f^2}}\sin\frac{\theta\sqrt{1+f^2}}{2}\sin\frac{\theta}{2}. \tag{7}$$

Under the small error approximation $|f| \ll 1$,

$$F_{\rm sf} \approx 1 - \frac{1}{2}\sin^2\left(\frac{\theta}{2}\right) f^2. \tag{8}$$

Equations (7) and (8) show that the detuning degrades the fidelity with a large effect at large rotation angle. The fidelity does not depend on φ, which means uniformity for all rotation axes in the x-y plane.

IV. GEOMETRIC ROTATION

In this section a geometric rotation is designed using A-A phase [18]. The rotation defined in Eq. (2) can be rewritten using a pair of orthogonal states $|\pm\rangle_\varphi$ as

$$U(\theta,\varphi)\,|\pm\rangle_\varphi = e^{\mp i\theta/2}\,|\pm\rangle_\varphi\,, \tag{9}$$

where $|\pm\rangle_\varphi = \frac{1}{\sqrt{2}}\begin{pmatrix}1\\ \pm e^{i\varphi}\end{pmatrix}$ are the eigenstates of operator $\vec{\sigma}\cdot\vec{n}$ represented by a pair of basis vectors parallel to the rotation axis $\vec{n}$ defined by angle φ in the x-y plane as shown in Fig. 1(b). An all-geometric scheme realizes the operation in Eq. (9) by making the two basis vectors go through closed loops to acquire the required phase terms. In order to ensure the phases are purely geometric in this process where the dynamic phase vanishes, the evolution loop for each of the basis vectors has to consist of segments of great circles on the Bloch sphere [20,30]. There are infinite options to design the loops to perform a given rotation, since the number of segments could be any value from 2 to infinity while making the solid angle enclosed by the loop to be the rotation angle θ. We focus our study on a three-segment loop, which is the simplest that an on-resonant field can drive. The loops for $|+\rangle_\varphi$ and $|-\rangle_\varphi$ are marked by the shaded areas A and B, respectively in Fig. 1(b), where every segment of the loops is made on a geodesic and the solid angle enclosed by the loop is the desired rotation angle. The field that drives the eigenvectors through the loops has three segments as well, with corresponding parameters denoted as $(\pi/2,\varphi+\pi/2)$, $(\pi,\varphi-\pi/2-\theta/2)$, and $(\pi/2,\varphi+\pi/2)$, where the first value in each parenthesis denotes the pulse area and the second value the phase. Driven by this field, basis vectors $|+\rangle_\varphi$ and $|-\rangle_\varphi$ go through their closed loops A and B in Fig. 1(b), respectively. While state $|+\rangle_\varphi$ gains a geometric phase of $-\theta/2$ becoming $e^{-i\theta/2}|+\rangle_\varphi$, state $|-\rangle_\varphi$ gains an opposite phase and turns into $e^{i\theta/2}|-\rangle_\varphi$. Under such an operation an arbitrary qubit state $|\psi\rangle = \begin{pmatrix}c_0\\ c_1\end{pmatrix}$ turns into

$$\begin{pmatrix}\cos\frac{\theta}{2}c_1 - ie^{-i\varphi}\sin\frac{\theta}{2}c_0\\ -ie^{i\varphi}\sin\frac{\theta}{2}c_1 + \cos\frac{\theta}{2}c_0\end{pmatrix}.$$

This is equivalent to applying a rotation operator in Eq. (2) to the initial state. On this geometric path the operation is accomplished by three consecutive rotations as

$$U(\theta,\varphi) = U(\pi/2,\varphi+\pi/2)U(-\pi,\varphi + \pi/2+\theta/2)U(\pi/2,\varphi+\pi/2). \tag{10}$$

Throughout the path the Rabi vectors are always perpendicular to the basis vectors, which nulls the dynamic phase change in the process.

In the presence of systematic errors in the pulse area and frequency detuning, the ideal operator in Eq. (10) turns into

$$V(\theta,\varphi) = V(\pi/2,\varphi+\pi/2)V(-\pi,\varphi + \pi/2+\theta/2)V(\pi/2,\varphi+\pi/2). \tag{11}$$

This operator is calculated by plugging in the imperfect pulse areas and/or axes in each of the segments. Then the fidelity can be calculated according to Eq. (3).

For the same percentage pulse area error ε as for the simple pulse operator, the fidelity of the geometric operator is calculated to be

$$F_{g\varepsilon} = \sin^2\frac{\pi\varepsilon}{2}\cos\frac{\theta}{2} + \cos^2\frac{\pi\varepsilon}{2}\cos^2\frac{\theta}{2} + \cos\frac{\pi\varepsilon}{2}\sin^2\frac{\theta}{2}. \tag{12}$$

The fidelity is a function of both pulse area error and rotation angle while the rotation axis is not involved. When the error is small,$|\varepsilon| \ll 1$, Eq. (12) approximates to

$$F_{g\varepsilon} \approx 1 - \frac{1}{2}\frac{1}{4}(\pi\varepsilon)^2\left[\cos\frac{\theta}{2} - 1\right]^2. \tag{13}$$

By comparing Eqs. (5) and (13), one can conclude, under the small error approximation, that the fidelity of the geometric operator is always equal to or better than the simple pulse operator. Both operators have 100% fidelity at $\theta = 0$, and a minimum fidelity, $1 - \frac{1}{2}\frac{1}{4}(\pi\varepsilon)^2$, at $|\theta| = \pi$. Other than those two points, the geometric operator always yields better fidelity. Beyond the small error regime, the comparison of the exact fidelities of the two operators is plotted in Fig. 2. The fidelity difference $F_{g\varepsilon} - F_{s\varepsilon}$ as a function of the percentage error and the rotation angle is plotted in Fig. 2(a) and the average of the fidelity over all rotation angles in Fig. 2(b). The results show that the geometric operator holds equal or higher fidelity compared to the simple pulse operator for all rotation angles and all values of pulse area error between 0 and 100%. As a result, the geometric operator has higher average fidelity than the simple pulse operator.

Similarly, the fidelity of the geometric operator is calculated in the presence of the frequency detuning error as

$$F_{\rm gf} = \frac{1}{1+f^2}\cos^2\frac{\theta}{2} + \frac{f^2}{1+f^2}\cos\frac{\theta}{2} + \frac{1}{\sqrt{1+f^2}}\sin^2\frac{\theta}{2}. \tag{14}$$

The small error approximation leads to

$$F_{\rm gf} \approx 1 - \frac{1}{2}f^2\left(\cos\frac{\theta}{2} - 1\right)^2. \tag{15}$$

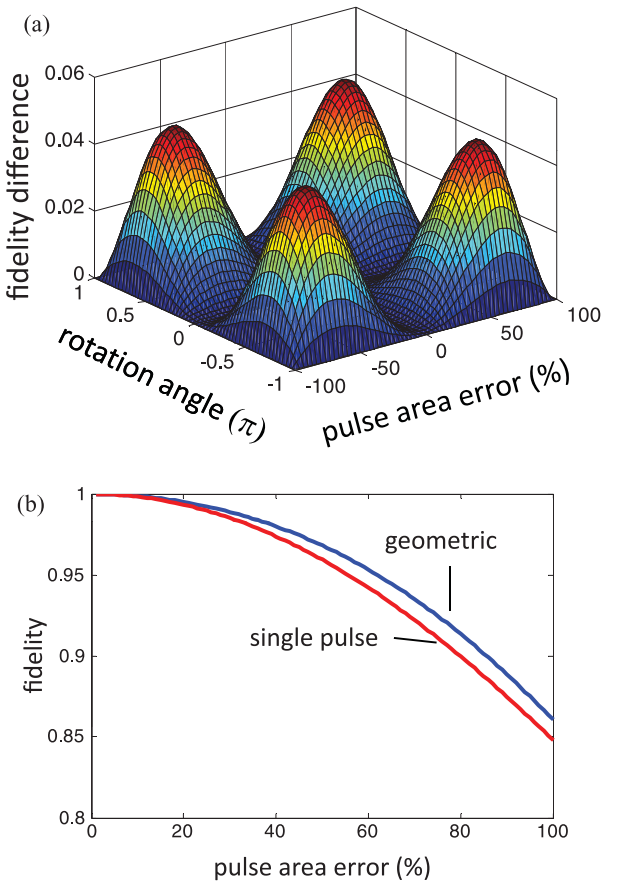

FIG. 2. (Color online) (a) Fidelity difference between geometric and simple pulse operators as a function of pulse area error and rotation angle. (b) Fidelities affected by pulse area error for geometric and simple pulse operators averaged over rotation angles from $-\pi$ to $-\pi$.

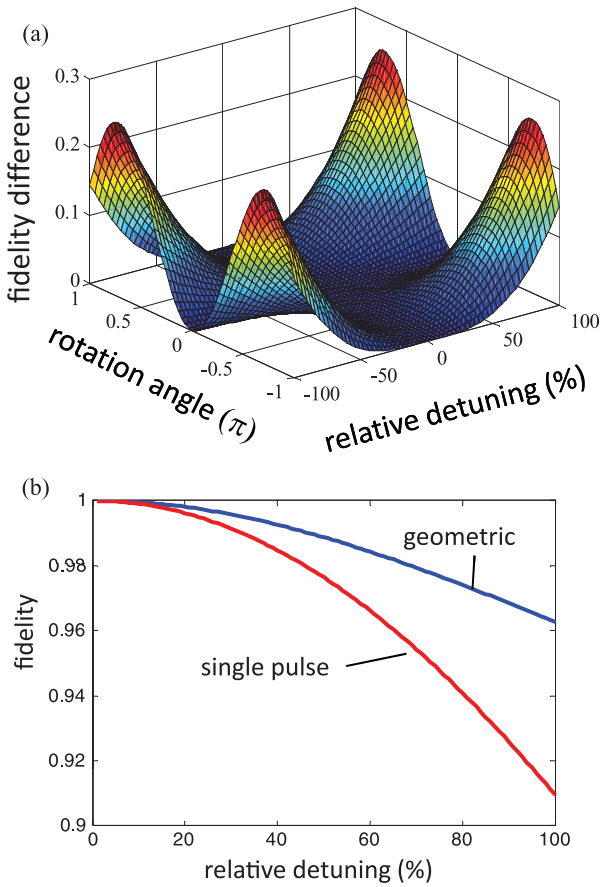

FIG. 3. (Color online) (a) Fidelity difference between geometric and simple pulse operators as a function of frequency detuning and rotation angle. (b) Fidelities affected by frequency detuning for geometric and simple pulse operators averaged over rotation angles from $-\pi$ to $-\pi$.

Under the condition $|f| << 1$, we compare the simple pulse operator in (8) and geometric operator in (15). For the rotation angle in the range of $0 < |\theta| < \pi$, $F_{\rm gf} > F_{\rm sf}$ holds true with the maximum fidelity $F_{\rm gf} = F_{\rm sf} = 1$ at $\theta = 0$, and the minimum fidelity $F_{\rm gf} = F_{\rm sf} = 1 - \frac{1}{2}f^2$ at $|\theta| = \pi$. The comparison of the two operators for large detuning range is presented in Fig. 3. The fidelity difference $F_{\rm gf} - F_{\rm sf}$ is plotted in Fig. 3(a). $F_{\rm gf}$ from Eq. (14) and $F_{\rm s\varepsilon}$ from Eq. (7) averaged over all rotation angles are plotted in Fig. 3(b). The results show that the geometric operator holds equal or higher fidelity compared to the simple pulse operator against the frequency detuning for all rotation angles.

The geometric operator, however, is not entirely immune to the systematic errors in the pulse area and detuning: the fidelity decreases when an error increases. Two consequences of a system error are noncyclic paths for the eigenvectors and nonvanishing dynamic phases. For practical reasons we keep to the small error regime so that the evolution paths for the eigenvectors $|\pm\rangle_\varphi$ can still be approximated as closed loops. As a result, the degradation of the operation fidelity caused by the erroneous Hamiltonian should be attributed to the dynamic phase. We calculated the dynamic phase according to $\alpha_d = -\frac{i}{\hbar}\int \langle\chi(t)|H|\chi(t)\rangle_\varphi dt$, where $|\chi(t)\rangle_\varphi$ represents the states evolving from the initial state $|+\rangle_\varphi$ on path A shown in Fig. 1(b). Under small pulse area error, $|\varepsilon| \ll 1$, the dynamic phase was calculated to be

$$\alpha_{\rm d\varepsilon} \approx \left(\frac{\pi}{2}\right)^2 \varepsilon \sin\frac{\theta}{2}\left(2 - \cos\frac{\theta}{2}\right). \tag{16}$$

This adds an extra angle $2|\alpha_{\rm d\varepsilon\pm}|$ to the desired rotation. Comparing Eqs. (13) and (16) reveals the relationship between the fidelity degradation and the dynamic phase as,

$$F_{\rm g\varepsilon} = 1 - \frac{2}{\pi^2}\frac{1-\cos\frac{\theta}{2}}{\left(1+\cos\frac{\theta}{2}\right)\left[2-\cos\frac{\theta}{2}\right]^2}\alpha_{\rm d\varepsilon}^2. \tag{17}$$

The second term shows the fidelity decreases quadratically with the dynamic phase caused by the pulse area error. A fidelity of 100% is achieved for a pure geometric operator, corresponding to a vanishing dynamic phase.

The fidelity degradation caused by the detuning was studied in a similar way. Under small error approximation, we calculated the dynamic phase as a function of the detuning and the rotation angle as

$$\alpha_{\rm df} \approx \frac{\pi}{2} f\left(\cos\frac{\theta}{2} - 1\right)^2. \tag{18}$$

Comparing the dynamic phase in (18) and the fidelity in (15), one can see the fidelity degradation is linked to the dynamic phase as

$$F_{\mathrm{gf}} = 1 - \frac{2}{\pi^2}\frac{1}{\left(\cos\frac{\theta}{2} - 1\right)^2}\alpha_{\mathrm{df}}^2, \tag{19}$$

which shows a similar relationship: the fidelity degrades quadratically with the dynamic phase caused by the frequency detuning.

While the rotation operator in Eq. (10) is all geometric under the ideal condition, systematic errors cause the eigenvectors to evolve on non-purely geometric paths. This is manifested as a nonvanishing dynamic phase. As a result, the operation fidelity decreases. This is consistent with the conclusion that the geometric path yields the highest fidelity.

V. CONCLUSION

A Bloch rotation operator based on nonadiabatic Abelian geometric phase has been designed and analyzed using a general model for a two-level qubit driven by a parameterized Hamiltonian. This operator is sufficient to make a set of universal single-qubit gates by setting the parameters such as pulse area, frequency, and phase of the effective control field. The fidelity of the geometric operator was analyzed against the systematic errors in the pulse area and the frequency detuning. An operator-based fidelity definition was used so that the results are independent of the qubit state. The geometric rotation operator was compared with the conventional simple pulse dynamic rotation. The systematic error degrades both types of operations with low fidelity at large rotation angle. The geometric operator shows overall improved fidelity over the simple pulse rotation. The reason for the degradation of the geometric operation is that the operator is no longer purely geometric when the systematic errors in both pulse area and frequency detuning cause the evolution path to deviate from the geometric path. As a result, the decrease in the fidelity is related to a nonvanishing dynamic phase. Further investigation is needed on the origin of the robustness of the geometric rotation against systematic errors compared with the dynamic operator.

Since our analysis is based on a generic nondegenerate two-level qubit model, the method and results in this paper are applicable to a variety of physical qubit systems, such as: NMR, atoms, ions, photons, superconducting circuits, and quantum dots. The model is suitable for both single-entity and ensemble qubits. When the inhomogeniety exists in the pulse area error or the frequency detuning in an ensemble, the fidelity calculation should be averaged over the entire ensemble. Geometric two-qubit gates, such as controlled-not and controlled-phase gates, can be analyzed in a similar way by introducing a qubit-qubit coupling term to the driving Hamiltonian.

While systematic control errors that can be parameterized into effective pulse area and frequency detuning errors exist in realistic systems, stochastic random fluctuation in the Hamiltonian is equally important. Both the dynamic and geometric operators discussed in this paper can be studied through numerical calculation of the fidelity according to Eq. (3), which is quite straightforward. However, the results will depend on the noise model, which could be quite different for the parameterized effective field in different physical systems and needs further investigation.

Our results on systematic errors are obtained for the simplest geometric path driven by an on-resonance effective field. More geometric paths can be designed by including off-resonance fields. For the practical purpose of achieving maximal gate fidelity, the path design should be optimized against both systematic and stochastic errors. The composition of the set of universal gates could play an important role as well in the optimization process.

ACKNOWLEDGMENTS

The authors gratefully acknowledge grant support from National Institute of Standards and Technology (Contract No. 70NANB7H6138, Am 001) and from the Office of Naval Research (Contract No. N00014-09-1-1025A). M.L. would like to thank Dr. Sophia Economou for fruitful discussions.

[1] D. Deutsch, Proc. R. Soc. London A **425**, 73 (1989).
[2] E. Knill, Nature **434**, 39 (2005).
[3] P. W. Shor, Phys. Rev. A **52**, R2493 (1995); A. M. Steane, Phys. Rev. Lett. **77**, 793 (1996).
[4] C. M. Dawson, H. L. Haselgrove, and M. A. Nielsen, Phys. Rev. Lett. **96**, 020501 (2006); R. Li, M. Hoover, and F. Gaitan, Quant. Info. Camp. **9**, 290 (2009).
[5] P. Zanardi and M. Rasetti, Phys. Lett. A **264**, 94 (1999).
[6] A. Recati, T. Calarco, P. Zanardi, J. I. Cirac, and P. Zoller, Phys. Rev. A **66**, 032309 (2002).
[7] J. Pachos and S. Chountasis, Phys. Rev. A **62**, 052318 (2000).
[8] X.-B. Wang and M. Keiji, Phys. Rev. Lett. **87**, 097901 (2001); J. A. Jones, V. Vedral, A. Ekert, and G. Castagnoli, Nature **398**, 305 (2002); Y. Ota, Y. Goto, Y. Kondo, and A. M. Nakahara, Phys. Rev. A **80**, 052311 (2009).
[9] L.-M. Duan, J. I. Cirac, and P. Zoller, Science **292**, 1695 (2001); F. Schmidt-Kaler, H. Haffner, M. Riebe, S. Gulde, G. P. T. Lancaster, T. Deuschle, C. Becher, C. F. Roos, J. Escher, and R. Blatt, Nature **422**, 408 (2003); D. Leibfried *et al.*, *ibid.* **422**, 412 (2003).
[10] J. J. Garcia-Ripoll and J. I. Cirac, Philos. Trans. R. Soc. London A **361**, 1537 (2003).
[11] G. Falci, R. Fazio, G. M. Palma, J. Siewert, and V. Vedral, Nature **407**, 355 (2000).
[12] M. Tian, Z. W. Barber, J. A. Fischer, and W. R. Babbitt, Phys Rev. A **69**, 050301(R) (2004); M. Tian, I. Zafarullah, T. Chang, R. K. Mohan, and W. R. Babbitt, *ibid.* **79**, 022312 (2009).
[13] S. E. Economou and T. L. Reinecke, Phys. Rev. Lett. **99**, 217401 (2007); S. Yin and D. M. Tong, Phys. Rev. A **79**, 044303 (2009).
[14] O. Oreshkov, T. A. Brun, and D. A. Lidar, Phys. Rev. Lett. **102**, 070502 (2009); O. Oreshkov, *ibid.* **103**, 090502 (2009).
[15] G. De Chiara and G. M. Palma, Phys. Rev. Lett. **91**, 090404 (2003); P. Solinas, P. Zanardi, and N. Zanghi, Phys. Rev. A **70**, 042316 (2004); C. Lupo, P. Aniello, M. Napolitano, and G. Florio, *ibid.* **76**, 012309 (2007).

[16] G. Florio, P. Facchi, R. Fazio V. Giovanetti, and S. Pascazio, Phys. Rev. A **73**, 022327(2006).
[17] M. V. Berry, Proc. R. Soc. London A **392**, 45 (1984).
[18] Y. Aharonov and J. Anandan, Phys. Rev. Lett. **58**, 1593 (1987).
[19] A. Nazir, T. P. Spiller, and W. J. Munro, Phys. Rev. A **65**, 042303 (2002).
[20] A. Blais and A. M. S. Tremblay, Phys. Rev. A **67**, 012308 (2003).
[21] S-L Zhu and P. Zanardi, Phys. Rev. A **72**, 020301(R) (2005).
[22] S. Fillipp, Eur. Phys. J. **160**, 165 (2008).
[23] M. A. Neilsen and I. L. Chuang, *Quantum Computation and Quantum Information* (Cambridge University Press, Cambridge, 2000).
[24] L. Allen and J. H. Eberly, *Optical Resonance, and Two-Level Atoms* (Dover Publications, Inc., New York, 1987).
[25] M. Nielsen, Phys. Lett. A **303**, 249 (2002); C. M. Dawson, H. L. Haselgrove, and M. A. Nielsen, Phys. Rev. A **73**, 052306 (2006).
[26] X. Wang, C-S. Yu, and X. X. Yi, Phys. Lett. A **373**, 58 (2008).
[27] M. H. Levitt, Prog. NMR Spectrosc. **18**, 61 (1986).
[28] R. Tycko, Phys. Rev. Lett. **51**, 775 (1983).
[29] J. A. Jones, Philos. Trans. R. Soc. London A **361**, 1429 (2003).
[30] E. Sjoqvist, Physics **1**, 35 (2008).